

# Could the LHC two-photon signal correspond to the heavier scalar in two-Higgs-doublet models?

P. M. Ferreira,<sup>1,2,\*</sup> Rui Santos,<sup>1,2,†</sup> Marc Sher,<sup>3,‡</sup> and João P. Silva<sup>1,4,§</sup>

<sup>1</sup>*Instituto Superior de Engenharia de Lisboa, 1959-007 Lisboa, Portugal*

<sup>2</sup>*Centro de Física Teórica e Computacional, Faculdade de Ciências, Universidade de Lisboa, Av. Prof. Gama Pinto 2, 1649-003 Lisboa, Portugal*

<sup>3</sup>*High Energy Theory Group, College of William and Mary, Williamsburg, Virginia 23187, U.S.A.*

<sup>4</sup>*Centro de Física Teórica de Partículas, Instituto Superior Técnico, Technical University of Lisbon, 1049-001 Lisbon, Portugal*

(Dated: November 29, 2018)

LHC has reported tantalizing hints for a Higgs boson of mass 125 GeV decaying into two photons. We focus on two-Higgs-doublet Models, and study the interesting possibility that the heavier scalar  $H$  has been seen, with the lightest scalar  $h$  having thus far escaped detection. Non-observation of  $h$  at LEP severely constrains the parameter-space of two-Higgs-doublet models. We analyze cases where the decay  $H \rightarrow hh$  is kinematically allowed, and cases where it is not, in the context of type I, type II, lepton-specific, and flipped models.

PACS numbers: 12.60.Fr, 14.80.Ec, 14.80.-j

## I. INTRODUCTION

After a decades-long wait, experiments at the LHC have finally started to probe the electroweak symmetry breaking sector of the electroweak theory. In the Standard Model, this entails a single scalar field whose particle remnant is the Higgs boson. There is no fundamental principle why the physical theory should involve only one scalar field, however. As is the case for fermions, scalars could appear in multiple families. The simplest such extension is the two-Higgs-doublet model (2HDM), recently reviewed in Ref. [1], where details and extensive references to the original literature may be found.

Generic 2HDMs exhibit flavor-changing neutral currents, for which there are stringent bounds arising from mixing in the neutral meson systems, such as  $K-\bar{K}$  and  $B_d-\bar{B}_d$ . The usual solution invokes a discrete  $Z_2$  symmetry. In the type I 2HDM, all fermions couple to a single Higgs doublet. The lepton-specific model is similar to type I, in that all quarks couple only to one Higgs doublet, but the leptons couple exclusively to the other Higgs doublet. In the type II 2HDM, up-type quarks and charged leptons couple to one Higgs doublet, while down-type quarks couple to the other. The flipped model is obtained from type II by flipping the leptons; up-type quarks couple to one Higgs doublet, while down-type quarks and leptons couple to the other.

LHC [2, 3] has reported some hints for a 125 GeV state decaying into two photons. In the context of 2HDMs, this state could be the light scalar  $h$ , the pseudoscalar particle  $A$ , or the heavy scalar  $H$ . Consequences of the first possibility were investigated in Ref. [4]; consequences of the second were discussed in Ref. [5]. Here we focus on the third possibility: that there is indeed a scalar particle of 125 GeV, but that this is the heavier of the two scalars,  $H$ . This would mean that the lightest scalar  $h$  should have, thus far, evaded detection. The combined requirements on  $H$  and  $h$  place stringent limits on the parameter space. We will consider two qualitatively distinct cases. In case 1,  $m_h = 105$  GeV and  $m_H = 125$  GeV, thus precluding the decay  $H \rightarrow hh$ . In case 2,  $m_h = 50$  GeV and  $m_H = 125$  GeV, implying that  $H \rightarrow hh$  is kinematically allowed. In both cases, we assume that the charged scalars and the neutral pseudoscalar are sufficiently heavy (or their couplings sufficiently suppressed) that they do not affect LHC data.

---

\*E-mail: ferreira@cii.fc.ul.pt

†E-mail: rsantos@cii.fc.ul.pt

‡E-mail: mtsher@wm.edu

§E-mail: jpsilva@cftp.ist.utl.pt

|             | Type I                     | Type II                     | Lepton-specific             | Flipped                     |
|-------------|----------------------------|-----------------------------|-----------------------------|-----------------------------|
| $htt$       | $\cos \alpha / \sin \beta$ | $\cos \alpha / \sin \beta$  | $\cos \alpha / \sin \beta$  | $\cos \alpha / \sin \beta$  |
| $hbb$       | $\cos \alpha / \sin \beta$ | $-\sin \alpha / \cos \beta$ | $\cos \alpha / \sin \beta$  | $-\sin \alpha / \cos \beta$ |
| $h\tau\tau$ | $\cos \alpha / \sin \beta$ | $-\sin \alpha / \cos \beta$ | $-\sin \alpha / \cos \beta$ | $\cos \alpha / \sin \beta$  |
| $Htt$       | $\sin \alpha / \sin \beta$ | $\sin \alpha / \sin \beta$  | $\sin \alpha / \sin \beta$  | $\sin \alpha / \sin \beta$  |
| $Hbb$       | $\sin \alpha / \sin \beta$ | $\cos \alpha / \cos \beta$  | $\sin \alpha / \sin \beta$  | $\cos \alpha / \cos \beta$  |
| $H\tau\tau$ | $\sin \alpha / \sin \beta$ | $\cos \alpha / \cos \beta$  | $\cos \alpha / \cos \beta$  | $\sin \alpha / \sin \beta$  |

TABLE I: Yukawa couplings of  $t, b, \tau$  to the neutral Higgs scalars,  $h$  and  $H$ , in the four different models, divided by the Standard Model couplings.

We follow Ref. [4] and plot the various experimental constraints in the  $(\sin \alpha, \tan \beta)$  plane. Here,  $\alpha$  is the rotation angle which diagonalizes the neutral scalar mass matrix, and the angle  $\beta$  is defined as

$$\tan \beta \equiv \frac{v_2}{v_1}, \quad (1)$$

where  $v_1$  and  $v_2$  are the vacuum expectation values of the two scalar doublets, and  $v \equiv (v_1^2 + v_2^2)^{1/2}$  is the Standard Model vacuum expectation value. The two parameters  $\alpha$  and  $\beta$  determine the interactions of the various Higgs fields with the vector bosons and (given the fermion masses) with the fermions.

In all four models, the coupling of the neutral Higgs  $h$  ( $H$ ) to the  $W$  and  $Z$  bosons is the same as in the Standard Model, multiplied by  $\sin(\beta - \alpha)$  ( $\cos(\beta - \alpha)$ ). The other relevant couplings are listed in Table I. In the type I and lepton specific models, on the one hand, and in the type II and flipped models at small  $\tan \beta$ , on the other, the production through gluon fusion is determined by the coupling to the top in the triangle loop. In contrast, in the type II and flipped models at large  $\tan \beta$ , the triangle with the bottom quark becomes relevant and may even exceed that with the top quark.

LEP experiments searched for associated production of a light Higgs up to masses around 115 GeV [6]. In 2HDMs, rates with  $hVV$  couplings ( $V = Z, W$ ) are suppressed by  $\sin^2(\beta - \alpha)$ , which the LEP data constrains to lie below  $\sim 0.2$  for  $m_h = 105$  GeV [6, 7]. This implies a very stringent constraint on the  $(\sin \alpha, \tan \beta)$  plane, shown for  $m_h = 105$  GeV as the light yellow shaded areas in Fig. 1. For  $m_h = 50$  GeV, LEP constrains  $\sin^2(\beta - \alpha)$  to lie below  $\sim 0.04$ ,

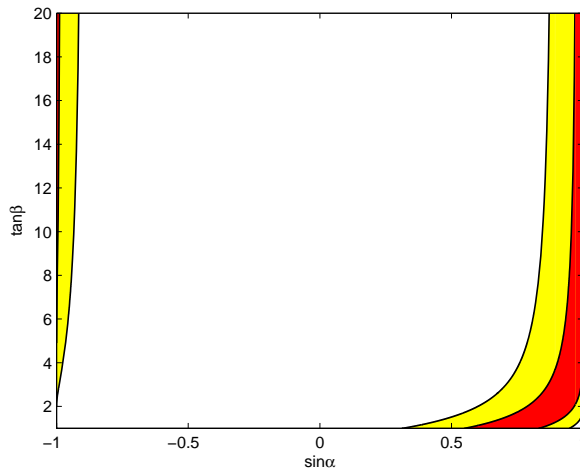


FIG. 1: We plot the lines of constant  $\sin^2(\beta - \alpha)$  in the  $(\sin \alpha, \tan \beta)$  plane. For  $m_h = 105$  GeV ( $m_h = 50$  GeV), LEP constrains the parameters to lie within the light yellow (dark red) shaded areas.

leading to even smaller allowed regions, shown in Fig. 1 as dark red areas.<sup>1</sup>

<sup>1</sup> Strictly speaking, the LEP constraint is even tighter in the exact fermiophobic limit of the type I model [8].

For the most part, the LEP constraint in Fig. 1 forces  $\sin \alpha$  to be close to  $\pm 1$  and  $\cos \alpha$  close to zero, with a severe impact on the observability of the lightest Higgs. Fig. 1 is easy to understand in the gaugephobic limit  $\alpha = \beta$ . In that case the  $hVV$  couplings vanish, satisfying trivially the LEP bound. For  $\tan \beta = 1$ ,  $\sin \alpha = 1/\sqrt{2}$ , which lies on the right hand allowed region in Fig. 1. Fig. 1 is also easy to understand in the large  $\tan \beta$  limit. In that case  $|\sin(\beta - \alpha)| \approx |\cos \alpha|$ , which the LEP limit forces to lie below  $\sqrt{0.2}$ , forcing  $|\sin \alpha| > \sqrt{0.8}$ , for  $m_h = 105$  GeV.

In the large  $\tan \beta$  limit, gluon-gluon fusion through the top triangle loop is suppressed by  $\cos \alpha$ , but production through vector boson fusion and associated production are also suppressed by  $\sin(\beta - \alpha)$ . Since the Standard Model predictions for the latter are much suppressed with respect to the former, we may ignore them. At the Tevatron, Higgs searches rely on associated production, so the  $W$  and  $Z$  can provide a tag for the events. As a result, the  $\sin^2(\beta - \alpha)$  suppression factor eliminates any useful Tevatron bounds on the Higgs mass (beyond the LEP bounds).

We define the number of  $H$  and  $h$  events relative to their Standard Model values, respectively by:

$$\begin{aligned}\eta_H &= \frac{N_H^{2HDM}}{N^{SM}}, \\ \eta_h &= \frac{N_h^{2HDM}}{N^{SM}},\end{aligned}\quad (2)$$

where  $N$  is the number of events, obtained through multiplication of the production cross section by the relevant branching ratio BR.

## II. $m_h$ ABOVE THE $H \rightarrow hh$ THRESHOLD

We begin with the type I model, where, for  $H \rightarrow \gamma\gamma$ , we find

$$\eta_H = \left(\frac{\sin \alpha}{\sin \beta}\right)^2 \frac{\text{BR}_H^{2HDM}}{\text{BR}^{SM}}. \quad (3)$$

The branching ratio in the Standard Model for a Higgs mass of 125.0 GeV is 0.00228 [9] with a 5% error.<sup>2</sup>

In Fig. 2a, we plot the  $\eta_H = 1/2$  and  $\eta_H = 1$  lines in the  $(\sin \alpha, \tan \beta)$  plane. Notice that it is difficult to exceed the

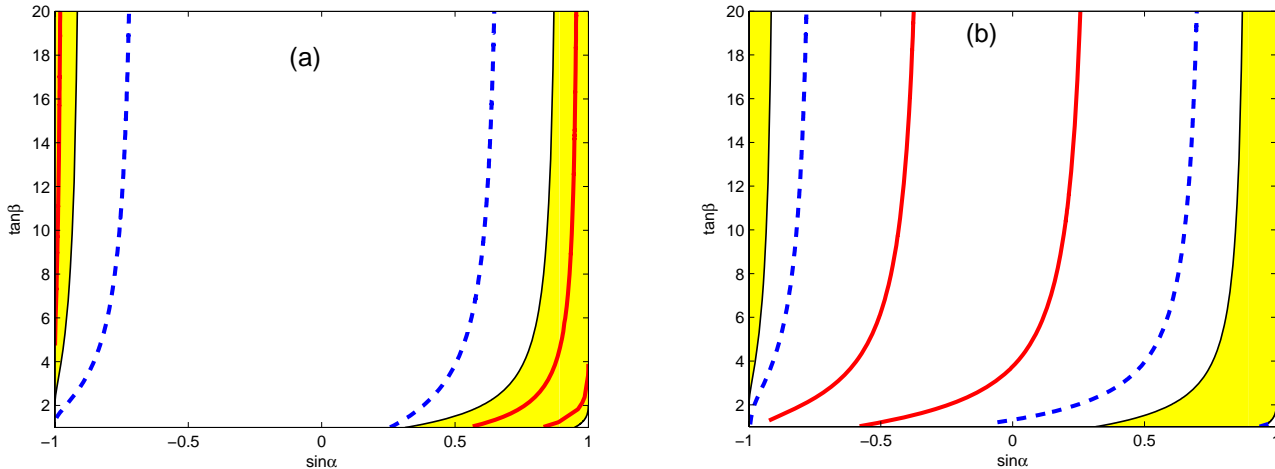


FIG. 2: For type I 2HDM, we plot the lines of equal ratios  $\eta_H = N_H^{2HDM}/N^{SM}$  (a) and  $\eta_h = N_h^{2HDM}/N^{SM}$  (b) in the  $(\sin \alpha, \tan \beta)$  plane for the  $H, h \rightarrow \gamma\gamma$  signal. Along the red (solid) lines the ratio is 1, and along the blue (dashed) lines it is  $1/2$ . The maximum  $\eta_H$  in the allowed region lies around 1.4.

Standard Model value in the context of type I models. We see that the LEP constraint on the light Higgs forces the

<sup>2</sup> Naturally, the precise position of the lines of constant  $\eta_H$  in the figures presented in this article will depend on the exact value taken for  $\text{BR}^{SM}$ . This also affects whether or not a line, for example  $\eta_H = 1$ , is allowed in some 2HDM. For consistency, we will take  $\text{BR}^{SM}$  directly from our programs. We are interested mainly in the qualitative features to be probed in the foreseeable future. Detailed higher order simulations will only be relevant once the precision of the experiments increases dramatically.

$\gamma\gamma$  decay of the heavy Higgs to lie very close to its SM value. For example,  $\eta_H = 1/2$  is excluded. This is consistent with its detectability in the  $\gamma\gamma$  channel at the LHC. For  $h \rightarrow \gamma\gamma$ , we find

$$\eta_h = \left( \frac{\cos \alpha}{\sin \beta} \right)^2 \frac{\text{BR}_h^{2HDM}}{\text{BR}^{SM}}, \quad (4)$$

which is plotted in Fig. 2b for  $\eta_h = 1/2$  and  $\eta_h = 1$ . All these values are excluded, meaning that, for this scenario, the lightest Higgs decay into  $\gamma\gamma$  will not be seen at LHC in the near future. As in  $\gamma\gamma$ , we find that  $H \rightarrow VV$  might be seen at rates comparable to the SM, while  $h \rightarrow VV$  cannot.

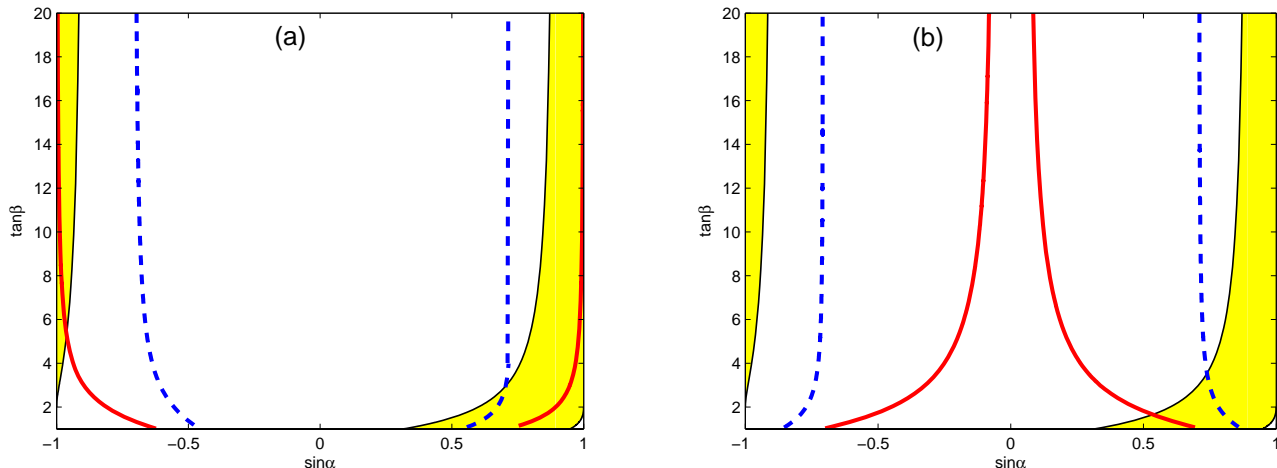


FIG. 3: For type I 2HDM, we plot the lines of equal ratios  $\eta_H = N_H^{2HDM}/N^{SM}$  (a) and  $\eta_h = N_h^{2HDM}/N^{SM}$  (b) in the  $(\sin \alpha, \tan \beta)$  plane for the  $H, h \rightarrow b\bar{b}$  signal. Along the red (solid) lines the ratio is 1, and along the blue (dashed) lines it is  $1/2$ . In the type I model,  $H, h \rightarrow \tau^+\tau^-$  exhibit very similar features.

An interesting situation for type I 2HDM arises in the decays into  $b\bar{b}$ , shown in Fig. 3. We find that  $H$  can decay into  $b\bar{b}$ , with  $\eta_H = 1$  or with  $\eta_H = 1/2$ , in a small region close to  $(\sin \alpha, \tan \beta) = (0.7, 2)$ . This is the same region in which  $h \rightarrow b\bar{b}$  could have the SM rate. The same conclusions hold for  $H \rightarrow \tau^+\tau^-$  and  $h \rightarrow \tau^+\tau^-$ , respectively. This raises the interesting possibility that the decays into  $b\bar{b}$  and  $\tau^+\tau^-$  could be sensitive to *both* the heavy and the light Higgs scalars, while only  $H$  can be seen in  $\gamma\gamma$  and  $VV$ .

A priori, the type II model has a different behavior, especially at large  $\tan \beta$ , due to the enhancement of the bottom quark Yukawa coupling, affecting both the production and decay of the Higgs. The production cross section for  $gg \rightarrow h$  was calculated with HIGLU [10]. Here the decay  $H \rightarrow \gamma\gamma$  can have  $\eta_H = 1/2, 1$  or even 2 in the regions of Fig. 1 consistent with the LEP constraint on  $h$ , but, again,  $h \rightarrow \gamma\gamma$  is undetectable. Similar conclusions occur for decays into  $VV$ . But the situation may improve with respect to the type I model, concerning  $b\bar{b}$ , as shown in Fig. 4. We see that both  $H \rightarrow b\bar{b}$  and  $h \rightarrow b\bar{b}$  could occur at rates *twice the SM rate*, for  $\sin \alpha > 0.8$  and  $\tan \beta > 13$ . The same behavior is seen in  $\tau^+\tau^-$ .

Next we consider the lepton-specific model. As in the type I model,  $h \rightarrow \gamma\gamma$  is unobservably small, while  $H \rightarrow \gamma\gamma$  may be detected. There is a subtle difference: improving the precision of the  $H \rightarrow \gamma\gamma$  measurement will imply a smaller region in the  $(\sin \alpha, \tan \beta)$  plane for the lepton-specific model than implied for the type I model. The same holds for  $VV$ . The decays into  $b\bar{b}$  have features similar to those for model I, shown in Fig. 3. In particular, detection of  $H \rightarrow b\bar{b}$  at SM rates is possible for large  $\sin \alpha$  and any value for  $\tan \beta$ , but simultaneous detection of  $h \rightarrow b\bar{b}$  around SM rates is only possible for low values of  $\tan \beta$ . Unlike model I, here the situation for decays into  $\tau^+\tau^-$  is very different from  $b\bar{b}$ , as shown in Fig. 5. We see that the decay into  $h \rightarrow \tau^+\tau^-$  could be substantially larger than in the SM, a point made in Refs. [4, 11]. Here we stress that such a large enhancement could occur for *both*  $H \rightarrow \tau^+\tau^-$  and  $h \rightarrow \tau^+\tau^-$ . The rate for  $H \rightarrow \tau^+\tau^-$  ( $h \rightarrow \tau^+\tau^-$ ) could even reach about ten (three) times the SM in the LEP allowed region. Thus, ATLAS and CMS are already starting to place upper limits on  $\tan \beta$  for a given  $\alpha$  in this model [12].

We now turn to the flipped model. Its  $\gamma\gamma$  and  $VV$  decay features follow those of the type II model. For the  $b\bar{b}$  events, we also re-obtain the type II model features, shown in Fig. 4, while the decays into  $\tau^+\tau^-$  follow instead Fig. 3, common to the  $b\bar{b}$  and  $\tau^+\tau^-$  channels in the type I model.

Finally, we notice that none of the conclusions on this section hinge on the presence or absence of a term in the Higgs potential softly breaking the discrete  $Z_2$  symmetry.

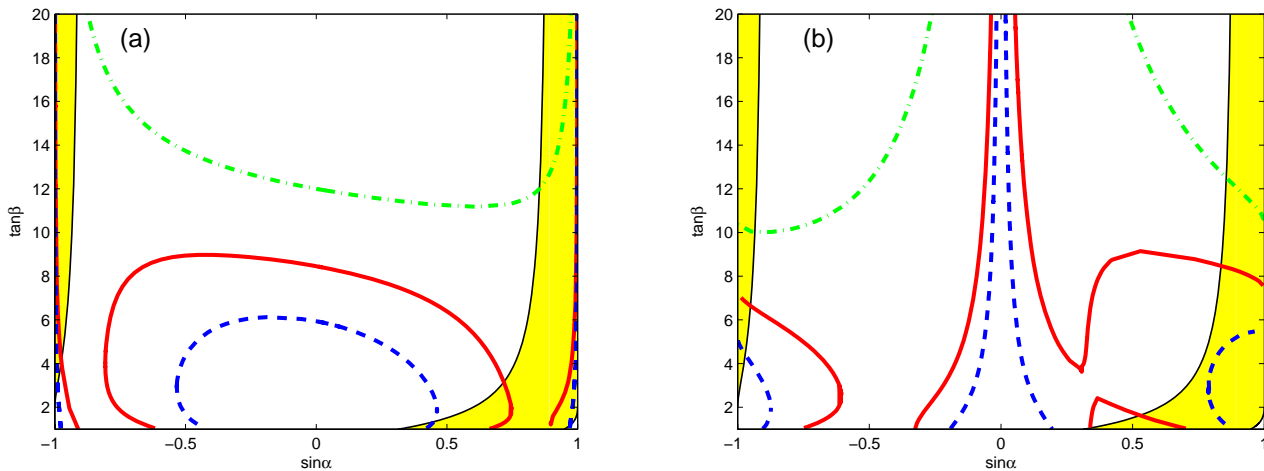


FIG. 4: For type II 2HDM, we plot the lines of equal ratios  $\eta_H = N_H^{2HDM}/N^{SM}$  (a) and  $\eta_h = N_h^{2HDM}/N^{SM}$  (b) in the  $(\sin \alpha, \tan \beta)$  plane for the  $H, h \rightarrow b\bar{b}$  signal. Along the red (solid) lines, the ratio is 1, along the blue (dashed) lines, it is 1/2, and along the green (dash-dotted) lines, it is 2.

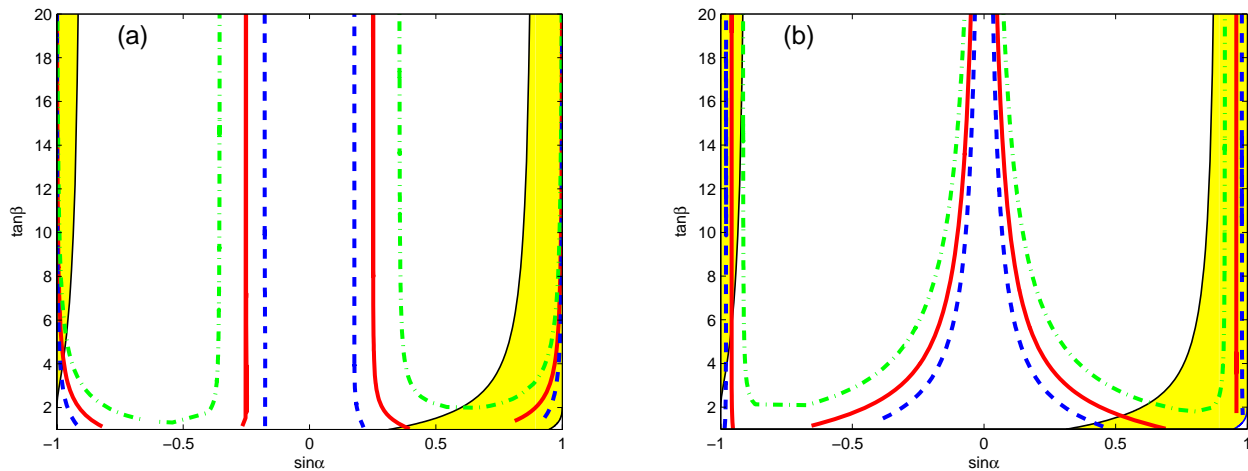


FIG. 5: For lepton specific 2HDM, we plot the lines of equal ratios  $\eta_H = N_H^{2HDM}/N^{SM}$  (a) and  $\eta_h = N_h^{2HDM}/N^{SM}$  (b) in the  $(\sin \alpha, \tan \beta)$  plane for the  $H, h \rightarrow \tau^+\tau^-$  signal. Along the red (solid) lines, the ratio is 1, along the blue (dashed) lines, it is 1/2, and along the green (dash-dotted) lines, it is 2.

### III. $m_h$ BELOW THE $H \rightarrow hh$ THRESHOLD

When  $H \rightarrow hh$  is kinematically allowed (such as in our second test case,  $m_H = 125$  GeV and  $m_h = 50$  GeV), we must consider the triple vertex [13, 14]

$$\lambda_{Hhh} \propto \frac{\cos(\beta - \alpha)}{\sin(2\beta)} (m_H^2 + 2m_h^2) \sin(2\alpha) \left[ 1 - x \left( \frac{3}{\sin(2\beta)} - \frac{1}{\sin(2\alpha)} \right) \right], \quad (5)$$

where

$$x = \frac{2\mu_{12}^2}{m_H^2 + 2m_h^2}, \quad (6)$$

and  $\mu_{12}^2$  allows for the inclusion in the Higgs potential of a possible term softly breaking the discrete  $Z_2$  symmetry.

### A. Without soft-breaking

We discuss the  $\mu_{12} = 0$  case in this section, leaving the  $\mu_{12} \neq 0$  case for the next section. Generically, when the  $H \rightarrow hh$  channel is opened, all other branching ratios are much suppressed and, in particular,  $H$  could not even be seen in the  $\gamma\gamma$  channel. This violates our working hypothesis that current LHC hints correspond indeed to  $H \rightarrow \gamma\gamma$ . As a result, we are interested in regions where  $\lambda_{Hhh}$  is close to zero. It is easy to find such regions in the  $(\sin\alpha, \tan\beta)$ , when  $\mu_{12} = 0$ . One may have  $\sin\alpha = -1, 0, 1$  or, from  $\cos(\beta - \alpha) = 0$ ,  $\beta = \alpha \pm \pi/2$ , leading to  $\tan\beta = -\sqrt{1 - \sin^2\alpha}/\sin\alpha$ . Of these, only the  $\sin\alpha \approx \pm 1$  regions are consistent with the  $\sin^2(\beta - \alpha) \lesssim 0.04$  LEP bound, shown as the dark red regions in Fig. 1. Therefore, it is only close to  $\sin\alpha \approx \pm 1$  that  $H$  may be visible in  $\gamma\gamma$ , or in any further channel other than  $H \rightarrow hh$ . However, this is a necessary but not a sufficient condition, since, in the regions consistent with small  $\lambda_{Hhh}$ , the couplings into the relevant channels might themselves be suppressed.

Fig. 6 shows  $\eta_H$  for the decay  $H \rightarrow \gamma\gamma$  for the type II and flipped models. This means that  $H \rightarrow \gamma\gamma$  may occur at

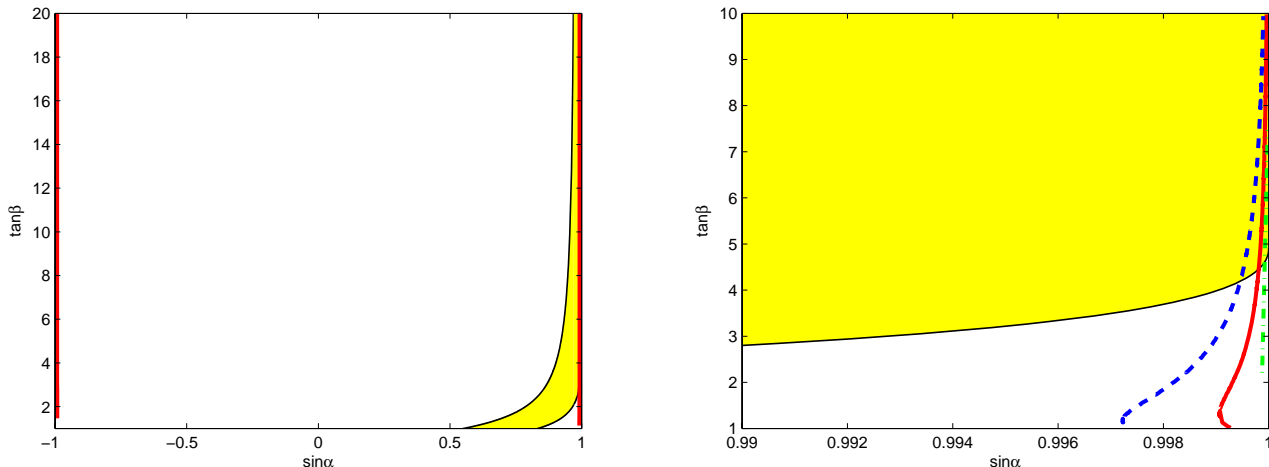


FIG. 6: For type II 2HDM, we plot the lines of equal ratios  $\eta_H = N_H^{2HDM}/N^{SM}$  in the  $(\sin\alpha, \tan\beta)$  plane for the  $H \rightarrow \gamma\gamma$  signal. With the scale shown on the left, the lines for  $\eta_H = 1/2, 1$  and  $2$  cannot be resolved. The leftmost allowed region is hidden by the red line. In the plot on the right we enlarge the region close to  $\sin\alpha = 1$ , with  $\eta_H = 1$  along the red (solid) line,  $\eta_H = 1/2$  along the blue (dashed) line, and  $\eta_H = 2$  along the green (dash-dotted) line. Notice that the light yellow region shown here corresponds to the dark red region in Fig. 1.

levels twice the SM, if and only if  $\sin\alpha \approx \pm 1$ , as predicted. Equivalent figures hold for the type I and lepton specific models, except that  $\eta_H$  may not exceed a value around the SM. The results are approximately the same for  $H \rightarrow VV$ . We conclude that all models are consistent with a 125 GeV  $H$  detected through its  $\gamma\gamma$  and  $VV$  decays, as long as  $\sin\alpha \approx \pm 1$ .

In the scenario under study in this section, the  $b\bar{b}$  and  $\tau^+\tau^-$  experiments turn out to be crucial to discriminate among the four models. Indeed, combining the LEP bound with the observability of  $H \rightarrow \gamma\gamma$ , we find the following  $H$  properties: it might be seen in both decays, for the type I model; it might be seen in  $b\bar{b}$  but not in  $\tau^+\tau^-$ , for the lepton specific model; it might be seen in  $\tau^+\tau^-$  but not in  $b\bar{b}$ , for the flipped model; and it will not be seen in either, for the type II model.

The  $\sin\alpha \approx \pm 1$  constraint also has a very strong impact on the detectability of the light scalar  $h$ . To avoid the LEP bound,  $\sin^2(\beta - \alpha) \lesssim 0.04$ , and  $h$  is close to gaugephobic. Thus, it cannot be seen in  $VV$ , regardless of the specific 2HDM considered. This also means that Higgs detection which requires associated production of a W or Z, as needed at the Tevatron, will be strongly suppressed. We have checked that  $h \rightarrow \gamma\gamma$  and  $h \rightarrow b\bar{b}$  is undetectable, while  $h \rightarrow \tau^+\tau^-$  is only detectable in the lepton specific model. Notice that, in the scenario  $m_H = 125$  GeV,  $m_h = 50$  GeV, and  $\mu_{12} = 0$ , the lepton specific model has a very interesting prediction:  $H$  may be seen in  $\gamma\gamma$ ,  $VV$ , and  $b\bar{b}$  at rates around the SM value, but it will not show up in  $\tau^+\tau^-$ , while  $h$  exhibits exactly the opposite features.

### B. With soft-breaking

As in the previous section, requiring  $H \rightarrow \gamma\gamma$  observability means that we are interested in regions where  $\lambda_{Hhh}$  is close to zero. Besides the conditions found in the previous section, where the pre-factor in Eq. (5) vanishes,  $\lambda_{Hhh}$  will

also vanish when

$$x = \frac{\sin(2\alpha)\sin(2\beta)}{3\sin(2\alpha) - \sin(2\beta)}. \quad (7)$$

Fig. 7 shows lines in the  $(\sin\alpha, \tan\beta)$  plane where the expression between squared parenthesis in Eq. (5) (and, thus,  $\lambda_{Hhh}$ ) vanishes.<sup>3</sup> Thus, at least in principle and given some chosen region in the  $(\sin\alpha, \tan\beta)$  plane, there is a

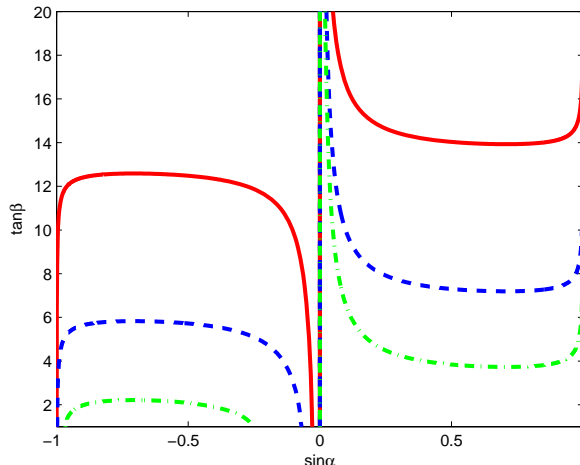


FIG. 7: Lines of constant  $x$  which satisfy Eq. (7):  $x = 0.05$  on the red (solid) line,  $x = 0.1$  on the blue (dashed) line,  $x = 0.2$  on the green (dash-dotted) line. Along these lines  $\lambda_{Hhh} = 0$ . Notice that the light yellow region shown here corresponds to the dark red region in Fig. 1.

judicious choice of  $\mu_{12}$  guaranteeing that  $H \rightarrow \gamma\gamma$  is not swamped by  $H \rightarrow hh$ . Notice that this is a necessary, but far from a sufficient condition, for  $H \rightarrow \gamma\gamma$  observability.

We conclude that, in the presence of  $\mu_{12} \neq 0$ , we might have  $H \rightarrow \gamma\gamma$  at levels consistent with LHC hints in regions away from the  $\sin\alpha = \pm 1$  constraints implied by Fig. 6. This is shown as a scatter plot in Fig. 8, drawn for the type II model and for random choices of  $\mu_{12}$ . One can now fill almost the entire LEP allowed region. This is even more so

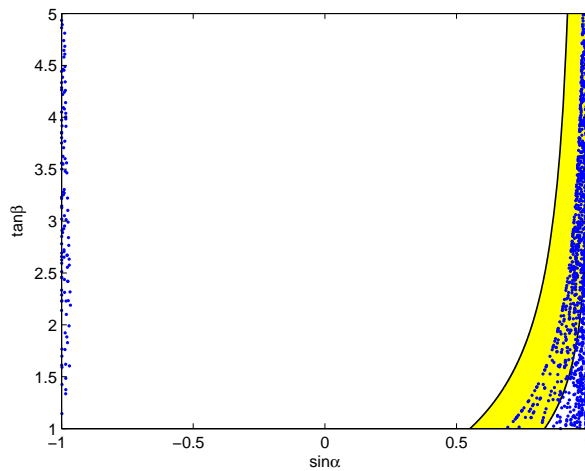


FIG. 8: Scatter plot for the  $H \rightarrow \gamma\gamma$  signal in the type II 2HDM, with  $\eta_H = N_H^{2HDM}/N^{SM} = 1$ . The allowed region on the left hand side of Fig. 1 is not shown because here we keep  $\tan\beta$  below 5.

in the type I model. In this case, the phenomenology is very similar to the  $m_h = 105$  GeV case.

<sup>3</sup> Some authors use  $M^2 = m_{12}^2/\sin(2\beta)$  instead of  $\mu_{12}^2$  [14]. A plot of lines with constant  $M^2$  will differ from Fig. 7, especially for negative  $\sin\alpha$ . Of course, the physics is the same.

#### IV. CONCLUSIONS

At long last, the experimental exploration of electroweak symmetry breaking has begun. The recent results at the LHC, if confirmed in the next few months, indicate that a scalar field exists at around 125 GeV which decays into two photons at a rate which is not very dissimilar to the Standard Model rate. It is natural to now begin discussing the consequences of such a field in the context of extensions to the Standard Model.

The simplest such extension is the two-Higgs doublet model, and we study the four versions of the model with natural flavor conservation. We address the question of whether the state at 125 GeV,  $H$ , could be the *heavier* of the two neutral scalars. For simplicity, we assume that the charged scalar and pseudoscalar are either sufficiently heavy or sufficiently decoupled that our results are not substantially affected. LEP's non-observation of a lighter Higgs,  $h$ , will severely constrain the parameter-space of the models, requiring the  $h$  to be nearly gaugephobic.

In all four models, we find that the decays  $h \rightarrow \gamma\gamma, WW, ZZ$  will be unobservable. If the  $h$  mass is above 62.5 GeV, then  $H \rightarrow hh$  is kinematically inaccessible. In the type I model, the decays of  $h$  and  $H$  into  $b\bar{b}$  and  $\tau^+\tau^-$  can both be observed at a rate similar to that of the Standard Model, whereas in the type II model, these decays can actually both occur at rates twice that of the Standard Model; we have delineated the parameter-space in both cases. In the lepton-specific case, one can have a huge enhancement in the  $H \rightarrow \tau^+\tau^-$  and  $h \rightarrow \tau^+\tau^-$  rates, the former (latter) possibly being enhanced by up to a factor of ten (three). The flipped model is similar to the type I and type II models.

If the  $h$  mass is below 62.5 GeV, the  $H \rightarrow hh$  is kinematically allowed, and will generally be large. We first study the case in which there is no term softly-breaking the  $Z_2$  symmetry which suppresses flavor-changing neutral currents. The observation of the two-photon decay at the LHC forces one into a small region of parameter-space in which the  $Hhh$  coupling is suppressed. Again, the two-photon decay of the  $h$  is undetectable, and in this region of parameter-space the  $b\bar{b}$  decay is also suppressed, as is  $\tau^+\tau^-$  in all but the lepton-specific model. In the lepton-specific model,  $h \rightarrow \tau^+\tau^-$  is detectable. With the soft-breaking term, the region of parameter-space in which the  $Hhh$  coupling is suppressed is substantially expanded, and can cover most of the LEP-allowed region, leading to similar results as in the heavier  $h$  case.

Should the LHC detect a second Higgs below the LEP bound decaying into  $\gamma\gamma$ , the two-Higgs doublet model will only be viable if the charged Higgs and pseudoscalar are quite light, so our assumption that they have no effect would break down. This, of course, would lead to more interesting phenomenology. Note that we have not discussed the possibility that the lighter Higgs is above the LEP bound (say at 119 GeV). Having the two neutral scalars so close in mass would require substantial fine tuning, but the possibility deserves further investigation.

#### Acknowledgments

We are grateful to Renato Guedes for help with HIGLU. The work of P.M.F., R.S., and J.P.S. is supported in part by the Portuguese *Fundação para a Ciência e a Tecnologia* (FCT) under contract PTDC/FIS/117951/2010 and by an FP7 Reintegration Grant, number PERG08-GA-2010-277025. P.M.F. and R.S. are also partially supported by PEST-OE/FIS/UI0618/2011. The work of M.S. is funded by the National Science Foundation grant NSF-PHY-1068008 and by a Joseph Plumeri Award. The work of J.P.S. is also funded by FCT through the projects CERN/FP/109305/2009 and U777-Plurianual, and by the EU RTN project Marie Curie: PITN-GA-2009-237920.

- 
- [1] G. C. Branco, P. M. Ferreira, L. Lavoura, M. N. Rebelo, M. Sher, and J. P. Silva, arXiv:1106.0034 [hep-ph].
  - [2] ATLAS collaboration, ATLAS note ATLAS-CONF-2011-161.
  - [3] CMS collaboration, talk given by G. Tonelli at CERN on Dec 13 2011.
  - [4] P. M. Ferreira, R. Santos, M. Sher, and J. P. Silva, arXiv:1112.3277 [hep-ph].
  - [5] G. Burdman, C. Haluch, and R. Matheus, arXiv:1112.3961 [hep-ph].
  - [6] R. Barate *et al.* [LEP Working Group for Higgs boson searches and ALEPH and DELPHI and L3 and OPAL Collaborations], Phys. Lett. B **565**, 61 (2003); S. Schael *et al.* [ALEPH and DELPHI and L3 and OPAL and LEP Working Group for Higgs Boson Searches Collaborations], Eur. Phys. J. C **47**, 547 (2006).
  - [7] P. M. Ferreira and D. R. T. Jones, JHEP **0908**, 069 (2009).
  - [8] LEP Collaborations (Aura Rosca for the collaboration), Presented at 31st International Conference on High Energy Physics (ICHEP 2002), Amsterdam, The Netherlands, 24-31 Jul 2002. Published in "Amsterdam 2002, ICHEP" 743-745, e-Print: hep-ex/0212038.
  - [9] A. Denner, S. Heinemeyer, I. Puljak, D. Rebuszi, and M. Spira, Eur. Phys. J. C **71**, 1753 (2011), arXiv:1107.5909 [hep-ph].
  - [10] M. Spira, arXiv:hep-ph/9510347.



- [11] A.G. Akeroyd, Phys. Lett. B **377**, 95 (1996).
- [12] CMS collaboration, preprint CMS-PAS-HIG-11-029 (2011); ATLAS, collaboration, G. Aad *et al.* arxiv:1107.5003 [hep-ex]; A. Arhrib, C. W. Chiang, D. K. Ghosh, and R. Santos, arXiv:1112.5527 [hep-ph].
- [13] M.N. Dubinin and A.V. Semenov, hep-ph/9812246.
- [14] S. Kanemura, Y. Okada, E. Senaha, C.-P. Yuan, Phys. Rev. D **70**, 115002 (2004).
- [15] A. Arhrib, R. Benbrik, R.B. Guedes, R. Santos, Phys. Rev. D **78**, 075002 (2008).